

Nonhelical inverse transfer of a decaying turbulent magnetic field

Axel Brandenburg,^{1,2,*} Tina Kahniashvili,^{3,4,5,†} and Alexander G. Tevzadze^{6,‡}

¹*Nordita, KTH Royal Institute of Technology and Stockholm University, Roslagstullsbacken 23, 10691 Stockholm, Sweden*

²*Department of Astronomy, AlbaNova University Center, Stockholm University, 10691 Stockholm, Sweden*

³*The McWilliams Center for Cosmology and Department of Physics,*

Carnegie Mellon University, 5000 Forbes Ave, Pittsburgh, PA 15213, USA

⁴*Department of Physics, Laurentian University, Ramsey Lake Road, Sudbury, ON P3E 2C, Canada*

⁵*Abastumani Astrophysical Observatory, Ilia State University,*

3-5 Cholokashvili Ave, Tbilisi, GE-0194, Georgia

⁶*Faculty of Exact and Natural Sciences, Tbilisi State University, 1 Chavchavadze Ave., Tbilisi, 0128, Georgia*

(Dated: April 9, 2014, Revision: 1.28)

In the presence of magnetic helicity, inverse energy transfer from small to large scales is well known in magnetohydrodynamic (MHD) turbulence and has important applications in astrophysics, cosmology, and fusion plasmas. Using high resolution direct numerical simulations, we report a similar inverse transfer even in nonhelical MHD turbulence. We compute for the first time spectral energy transfer rates to show that the inverse transfer is about half as strong as with helicity, but in both cases the magnetic gain at large scales results from velocity at similar scales interacting with smaller-scale magnetic fields. We argue that in both cases, the inverse transfer is a consequence of the universal k^4 and k^2 subinertial range spectra for magnetic and kinetic energies, respectively. The shallower k^2 spectrum forces the magnetic field to attain larger-scale coherence. The inertial range shows a clear k^{-2} spectrum and is the first example of fully isotropic magnetically dominated MHD turbulence exhibiting weak turbulence scaling.

PACS numbers: 98.70.Vc, 98.80.-k

The nature of magnetohydrodynamic (MHD) turbulence has received significant attention in recent years [1]. Whenever plasma is ionized, it is electrically conducting and the celebrated Kolmogorov turbulence theory [2] has to be replaced by an appropriate theory for MHD turbulence [3]. This becomes relevant under virtually all astrophysical circumstances. However, the universal character of MHD turbulence is debated and several fundamental questions remain unanswered: are kinetic and magnetic energy spectra similar and do they both show a $k^{-5/3}$ power law behavior with wavenumber k ? How does this depend on the magnetic Prandtl number, $\text{Pr}_M = \nu/\eta$, i.e., the ratio of kinematic viscosity and magnetic diffusivity? What is the role of the Alfvén effect, i.e., how does the presence of a finite Alfvén speed v_A enter the expression for the turbulent energy spectrum?

If the spectral properties of MHD turbulence are governed solely by the rate of energy transfer ϵ , we know already from dimensional arguments that the spectrum must scale as $E(k) \sim \epsilon^{2/3} k^{-5/3}$. In fact, MHD turbulence becomes increasingly anisotropic toward small scales [4] so the spectrum $E(k_\perp, k_\parallel)$ depends on the wavenumbers perpendicular and parallel to the magnetic field \mathbf{B} , and is essentially given by $\epsilon^{2/3} k_\perp^{-5/3}$, so most of the energy cascades perpendicular to \mathbf{B} .

Over the past ten years, this model has received signif-

icant support from direct numerical simulations (DNS) [1, 5, 6]. This also applies to the case when the magnetic field is not imposed, but generated self-consistently by the turbulent velocity \mathbf{u} through dynamo action [7]. However, when \mathbf{B} is decaying, the result may be sensitive to initial conditions and depend on the ratio v_A/u_{rms} of root mean square (rms) Alfvén speed and rms turbulent velocity. Recent DNS [8] found numerical evidence for three different scalings: Iroshnikov–Kraichnan scaling [9] proportional to $(\epsilon v_A)^{1/2} k^{-3/2}$ for $v_A/u_{\text{rms}} = 0.9$, Goldreich–Sridhar scaling [4] proportional to $\epsilon^{2/3} k_\perp^{-5/3}$ for $v_A/u_{\text{rms}} = 1.3$, and weak turbulence scaling [10] proportional to $(\epsilon v_A k_\parallel)^{1/2} k_\perp^{-2}$ for $v_A/u_{\text{rms}} = 2.0$; see Ref. [11] for a comparison of those three scalings. However, the physical interpretations of these results are subject to criticism in that dynamic alignment between \mathbf{u} and \mathbf{B} can be responsible for the shallower $k^{-3/2}$ scaling [5] and that the k^{-2} scaling could also be caused by a dominance of discontinuities [12].

In most previous studies, it has been taken for granted that for non-helical turbulence, energy is cascading toward small scales. An inverse cascade has so far only been found for helical turbulence [3, 13] and was confirmed in DNS [14, 15]. It is evident that such investigations require significant scale separation, i.e., the computational domain must be large enough to accommodate wavelengths much longer than the energy-carrying scale corresponding to the wavenumber of the location of the peak k_0 . Since an inverse transfer was not expected to occur in the absence of helicity, most previous work did not allow for sufficient scale separation. However, when there

*Electronic address: brandenb@nordita.org

†Electronic address: tinatin@phys.ksu.edu

‡Electronic address: aleko@tevza.org

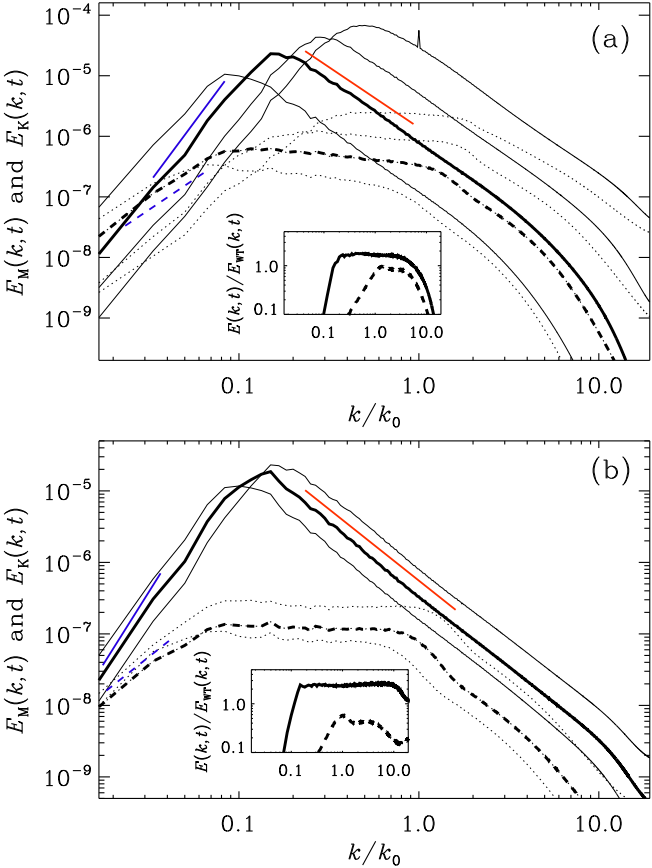


FIG. 1: (Color online) (a) Magnetic (solid lines) and kinetic (dashed lines) energy spectra for Run A at times $t/t_0 = 2, 14, 50$, and 200 ; the time $t/t_0 = 50$ is shown as bold lines. The straight lines indicate the slopes k^4 (solid, blue), k^2 (dashed, blue), and k^{-2} (red, solid). (b) Same for Run B, at $t/t_0 = 60, 140$, and 200 , with $t/t_0 = 140$ shown as bold lines.

is moderate scale separation, some inverse cascading was already found in the work of Ref. [14]. The present work shows that this behavior is genuine and becomes more pronounced at higher resolution, larger Reynolds numbers and larger scale separation.

We solve the compressible MHD equations for \mathbf{u} , the gas density ρ at constant sound speed c_s , and the magnetic vector potential \mathbf{A} , so $\mathbf{B} = \nabla \times \mathbf{A}$. Following our earlier work [16–18], we initialize our decaying DNS by restarting them from a snapshot of a driven DNS, where a random forcing was applied in the evolution equation for \mathbf{A} rather than \mathbf{u} . To allow for sufficient scale separation, we apply the forcing at wavenumber $k_0/k_1 = 60$, where k_1 is the smallest wavenumber that fits into the domain. We use the PENCIL CODE [19] at a resolution of 2304^3 meshpoints on 9216 processors. The code uses sixth order finite differences and a third order accurate time stepping scheme.

In Fig. 1 we show magnetic and kinetic energy spectra for Runs A and B with $\text{Pr}_M = 1$ and 10 , respec-

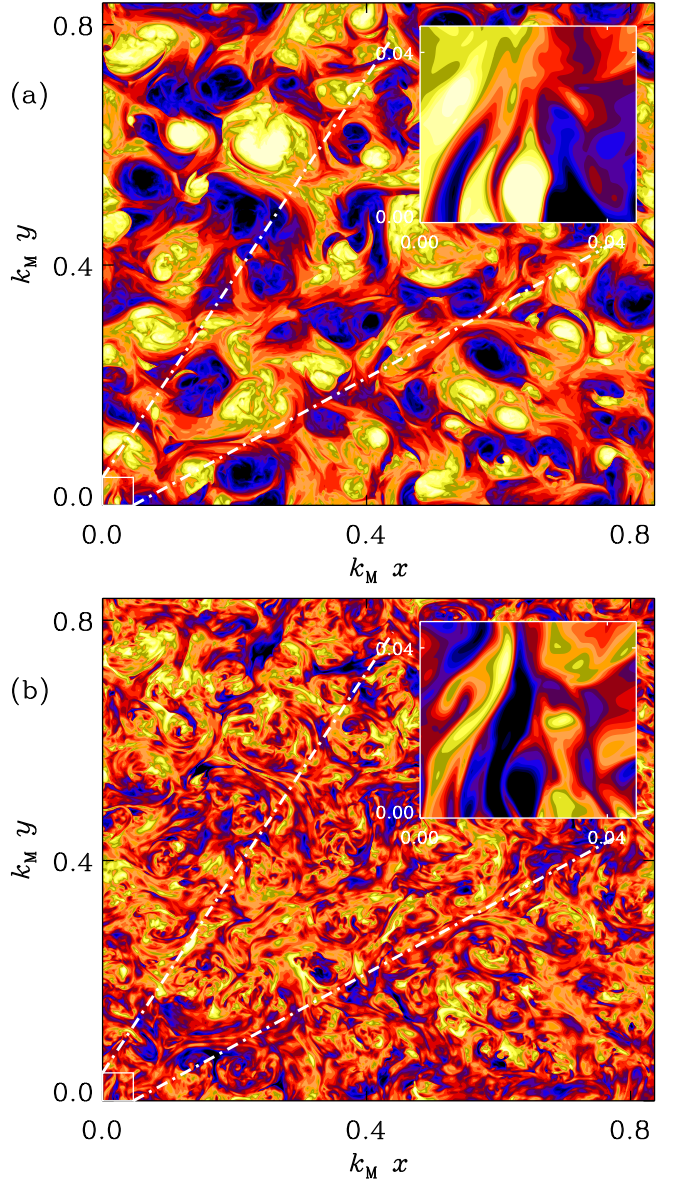


FIG. 2: (Color online) Contours of (a) $B_z(x, y)$ and (b) $u_z(x, y)$ for Run A. The insets show a zoom into the small square in the lower left corner.

tively, and in Fig. 2 slices $B_z(x, y)$ and $u_z(x, y)$ at $z = 0$ at the last time Run A, where time is given in units of the initial time t_0 . The spectra are normalized such that $\int E_M(k, t) dk = \mathcal{E}_M(t) = v_A^2/2$ and $\int E_K(k, t) dk = \mathcal{E}_K(t) = u_{\text{rms}}^2/2$ are magnetic and kinetic energies per unit mass. We find an inertial range with weak turbulence scaling,

$$E_{\text{WT}}(k, t) = C_{\text{WT}}(\epsilon v_A k_M)^{1/2} k^{-2}, \quad (1)$$

where $k_M^{-1}(t) = \int k^{-1} E_M(k, t) dk / \mathcal{E}_M(t)$ is the integral scale and has been used in place of k_{\parallel} . The prefactor is $C_{\text{WT}} \approx 1.9$ for $\text{Pr}_M = 1$ and ≈ 2.4 for $\text{Pr}_M = 10$, which was restarted from Run A at $t/t_0 = 50$.

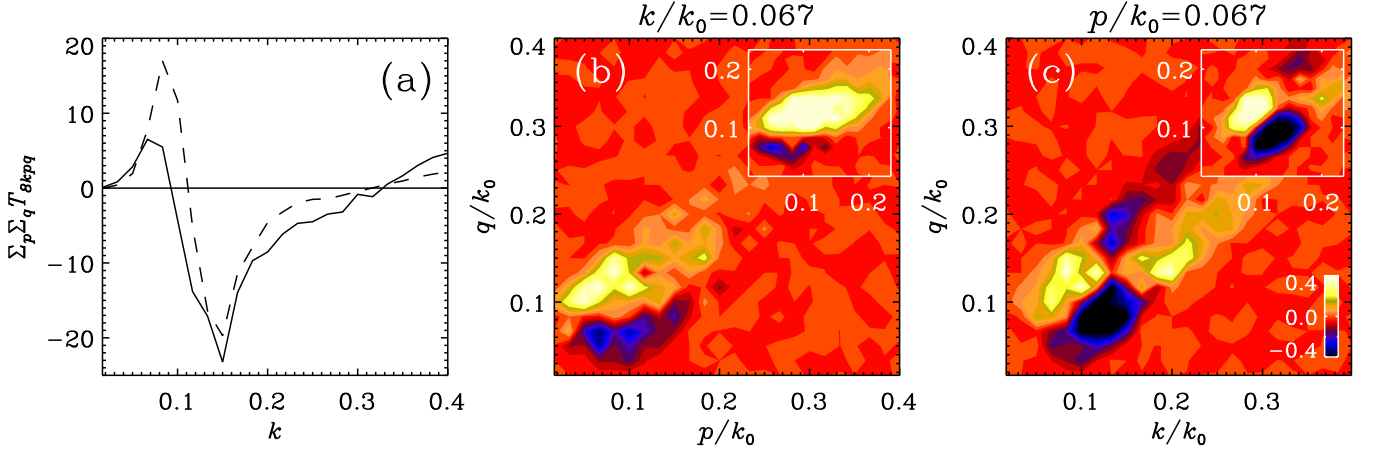


FIG. 3: (Color online) Spectral transfer function T_{kpq} , (a) as a function of k and summed over all p and q , (b) as a function of p and q for $k/k_1 = 4$, and (c) as a function of k and q for $p/k_1 = 4$. The dashed line in (a) and the insets in (b) and (c) show the corresponding case for a DNS with helicity; both for $\text{Pr}_M = 1$.

At small wavenumbers there are k^4 and k^2 subinertial ranges for $E_M(k, t)$ and $E_K(k, t)$, respectively. The k^4 Batchelor spectrum is in agreement with the causality requirement for a divergence-free vector field [20, 21]. On the other hand, there is no zero-divergence requirement for the velocity field, and this allows for the possibility to have a white noise spectrum for the velocity field, i.e. $E_K(k) \propto k^2$ [21]. The resulting difference in the scaling is also the reason that, even though magnetic energy dominates over kinetic, the two spectra must cross at sufficiently small wavenumbers.

To quantify the nature of inverse transfer we show in Fig. 3 representations of the spectral transfer function $T_{kpq} = \langle \mathbf{J}^k \cdot (\mathbf{u}^p \times \mathbf{B}^q) \rangle$ and compare with the corresponding helical case of Ref. [18], but with 1024^3 mesh points and at a comparable time. Here, the superscripts indicate the radius of a shell in wavenumber space of Fourier filtered vector fields; see Ref. [15] for such an analysis in driven helical turbulence. The transfer function T_{kpq} quantifies the gain of magnetic energy at wavenumber k from interactions of velocities at wavenumber p and magnetic fields at wavenumber q . Fig. 3(a) shows a gain for $k/k_0 < 0.1$, which is about half of that for the helical case. The corresponding losses for $k/k_0 > 0.1$ are about equal in the two cases. In both cases, the magnetic gain at $k/k_0 = 0.067 = 4/60$ results from \mathbf{u}^p with $0 < p/k_0 < 0.2$ interacting with \mathbf{B}^q at $q/k_0 > 0.1$; see the light yellow shades in Fig. 3(b). Note that work done by the Lorentz force is $\langle \mathbf{u}^p \cdot (\mathbf{J}^k \times \mathbf{B}^q) \rangle = -T_{kpq}$. Thus, negative values of T_{kpq} quantify the gain of *kinetic* energy at wavenumber p from interactions of magnetic fields at wavenumbers k and q . Blue dark shades in Fig. 3(c) indicate therefore that the gain of kinetic energy at $p/k_0 = 0.067$ results from magnetic interactions at wavenumbers k and q of around $0.1 k_0$. These results support the interpretation that the increase of spectral power at large scales is sim-

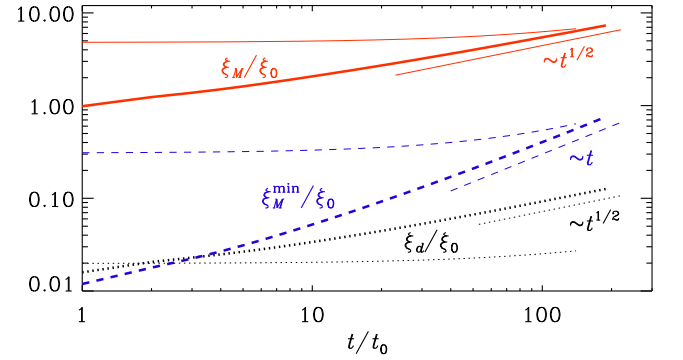


FIG. 4: Time evolution of $\xi_M = k_M^{-1}$ and ξ_M^{\min} , as well as ξ_d . Fat (thin) lines are for Run A (B).

ilar to the inverse cascade in the helical case.

To exclude that the inverse energy transfer is not a consequence of the invariance of magnetic helicity, $\mathcal{H}_M(t) = \langle \mathbf{A} \cdot \mathbf{B} \rangle$, we compare in Fig. 4 the magnetic integral scale $\xi_M = k_M^{-1}$ with its lower bound, $\xi_M^{\min} = |\mathcal{H}_M|/2\mathcal{E}_M$ [17]. Even though the initial condition was produced with non-helical plane waves, we find $\mathcal{H}_M \neq 0$ due to the effect of fluctuations. Since \mathcal{H}_M is conserved and \mathcal{E}_M decays like t^{-1} , ξ_M^{\min} grows linearly and faster than $\xi_M \sim t^{1/2}$, so they will eventually meet and then continue to grow as $t^{-2/3}$ [3, 17].

During the course of the simulation, the gap between ξ_M and ξ_M^{\min} has shrunk from about two to one order of magnitude (Fig. 4). However, to close the gap completely and thus to reach a fully helical state, one would need to extend the time by another two orders of magnitude (until $t/t_0 = 10^4$). It is therefore clear that helicity effects do not yet play a role in our DNS.

The energy is dissipated both viscously and resistively at rates ϵ_K and ϵ_M , respectively. It is instructive to com-

TABLE I: Comparison of relative dissipation rates, energies and other parameters for the two simulations discussed. Here, $\mathcal{E} = \mathcal{E}_M + \mathcal{E}_K$.

Run	Pr_M	ϵ_K/ϵ_M	ϵ_M/ϵ	ϵ_K/ϵ	$\mathcal{E}_M/\mathcal{E}$	$\mathcal{E}_K/\mathcal{E}$	Lu	Re
A	1	0.52	0.66	0.34	0.885	0.115	860	310
B	10	0.93	0.52	0.48	0.958	0.042	8900	185

pare these two rates. Since $\mathcal{E}_K \ll \mathcal{E}_M$, the dissipated energy comes predominantly from $-d\mathcal{E}_M/dt$, and yet a substantial fraction of it is used to drive kinetic energy by performing work on the Lorentz force. As a result, the viscously dissipated energy is substantial: $\epsilon_K/\epsilon_M = 0.5$ for $Pr_M = 1$ and 0.9 for $Pr_M = 10$ (Table I). This is qualitatively similar to hydrodynamically driven turbulence, where a somewhat steeper relation was found for $Pr_M < 1$: $\epsilon_K/\epsilon_M \propto Pr_M^{0.6}$ [22]. However, while the Reynolds number $Re = u_{rms}/\nu k_M$ takes only moderate values, the Lundquist number $Lu = v_A/\eta k_M$ is rather large for Run B and therefore uncertain. This probably also explains why Run B did not reach asymptotic scaling in Fig. 4.

In summary, we have shown that inverse transfer is a ubiquitous phenomenon of both helical and non-helical MHD. For helical MHD, this has been well known for nearly four decades [13], but for nonhelical MHD there have only been some low resolution DNS [14, 18]. Our new high resolution DNS now confirm the earlier hypothesis [18] that this inverse transfer is accomplished through small-scale magnetic field interacting with larger-scale velocity. We further show that at large enough length scales, kinetic energy always dominates over magnetic owing to the shallower k^2 spectrum of kinetic energy, which we show is responsible for inverse transfer both in helical and in nonhelical MHD. This is significant for cosmology and astrophysics, with applications not only to primordial magnetic fields, but also to ejecta from young stars, supernovae, and active galactic nuclei [23].

Our results are also important from a turbulence point of view in that they confirm the existence of the weak turbulence k^{-2} scaling for a strong magnetic field that is here globally isotropic and not an imposed one [6]. Furthermore, the velocity spectrum shows an extended plateau around the position of the magnetic peak and may be important for producing observationally detectable broad gravitational wave spectra [24].

We appreciate useful discussions with A. Neronov. Computing resources have been provided by the Swedish National Allocations Committee at the Center for Parallel Computers at the Royal Institute of Technology in Stockholm and by the Carnegie Mellon University supercomputer center. We acknowledge partial support from the Swedish Research Council grants 621-2011-5076 and 2012-5797, the European Research Coun-

cil AstroDyn Research Project 227952, the FRINATEK grant 231444 under the Research Council of Norway, the Swiss NSF grant SCOPE IZ7370-152581, the NSF grant AST-1109180, and the NASA Astrophysics Theory Program grant NNX10AC85G. A.B. and A.T. acknowledge the hospitality of the McWilliams Center for Cosmology where part of this work has been designed.

-
- [1] W. H. Matthaeus, S. Ghosh, S. Oughton, and D. A. Roberts, J. Geophys. Res. **101**, 7619 (1996); J. Cho and E.T. Vishniac, Astrophys. J. **538**, 217 (2000); J. Maron and P. Goldreich, Astrophys. J. **554**, 1175 (2001); W.-C. Müller, D. Biskamp, and R. Grappin, Phys. Rev. E **67**, 066302 (2003); A. Beresnyak, Phys. Rev. Lett. **106**, 075001 (2011).
 - [2] A. Kolmogorov, Doklady Akademii Nauk SSSR, **30**, 301 (1941); Doklady Akademii Nauk SSSR, **32**, 16 (1941).
 - [3] D. Biskamp, *Magnetohydrodynamic Turbulence* (Cambridge: Cambridge Univ. Press) 2003.
 - [4] P. Goldreich and S. Sridhar, Astrophys. J. **438**, 763 (1995).
 - [5] J. Mason, F. Cattaneo, and S. Boldyrev, Phys. Rev. Lett. **97**, 255002 (2006).
 - [6] J.C. Perez and S. Boldyrev, Astrophys. J. Lett. **672**, L61 (2008).
 - [7] N. E. L. Haugen, A. Brandenburg, and W. Dobler, Phys. Rev. E **70**, 016308 (2004).
 - [8] E. Lee, M. E. Brachet, A. Pouquet, P. D. Mininni, D. Rosenborg, Phys. Rev. E **81**, 016318 (2010).
 - [9] R. S. Iroshnikov, Sov. Astron. **7**, 566 (1963); R. H. Kraichnan, Phys. Fluids **8**, 1385 (1965).
 - [10] S. Galtier, S.V. Nazarenko, A.C. Newell, and A. Pouquet, J. Plasm. Phys. **63**, 447 (2000).
 - [11] A. Brandenburg and Å. Nordlund, Rep. Prog. Phys. **74**, 046901 (2011).
 - [12] V. Dallas and A. Alexakis, arXiv:1312.7336 (2013).
 - [13] A. Pouquet, U. Frisch, and J. Léorat, J. Fluid Mech. **77**, 321 (1976).
 - [14] M. Christensson, M. Hindmarsh, and A. Brandenburg, Phys. Rev. E **70**, 056405 (2001).
 - [15] A. Brandenburg, Astrophys. J. **550**, 824 (2001).
 - [16] T. Kahnashvili, A. Brandenburg, A. G. Tevzadze and B. Ratra, Phys. Rev. D **81**, 123002 (2010).
 - [17] A. G. Tevzadze, L. Kisslinger, A. Brandenburg and T. Kahnashvili, Astrophys. J. **759**, 54 (2012)
 - [18] T. Kahnashvili, A. G. Tevzadze, A. Brandenburg and A. Neronov, Phys. Rev. D **87**, no. 8, 083007 (2013); note that in their Eq. (14), v/η should read $\partial v/\partial \eta$.
 - [19] <http://pencil-code.googlecode.com/>
 - [20] R. Durrer and C. Caprini, JCAP **0311**, 010 (2003).
 - [21] P. A. Davidson, *Turbulence* (Oxford: Oxford University Press, 2004).
 - [22] A. Brandenburg, Astrophys. J. **697**, 1206 (2009); Astrophys. J. **741**, 92 (2011); Astron. Nachr. **332**, 51 (2011).
 - [23] A. M. Beck, K. Dolag, H. Lesch, and P. P. Kronberg, Mon. Not. R. Astron. Soc. **435**, 3575 (2013).
 - [24] T. Kahnashvili, L. Campanelli, G. Gogoberidze, Y. Maravlin, and B. Ratra, Phys. Rev. D **78**, 123006 (2008).